

Suppression of Capillary Wave Broadening of Interfaces in Binary Alloys due to Elastic Interactions

B. J. Schulz,¹ B. Dünweg,² K. Binder,¹ and M. Müller^{1,3}

¹*Institut für Physik, WA331, Johannes Gutenberg-Universität, Staudingerweg 7, D-55099 Mainz, Germany*

²*Max Planck Institute for Polymer Research, Ackermannweg 10, D-55128 Mainz, Germany*

³*Department of Physics, University of Wisconsin-Madison, 1150 University Avenue, Madison, Wisconsin 53706-1390, USA*

(Received 3 December 2004; published 24 August 2005)

By Monte Carlo simulations in the constant-temperature–constant-pressure ensemble a planar interface between unmixed *A*-rich and *B*-rich phases of a binary (*A*, *B*) alloy on a compressible diamond lattice is studied. No significant capillary wave broadening of the concentration profile across the interface is observed, unlike lattice models of incompressible mixtures and fluids. The distortion of the lattice structure across the interface is studied.

DOI: 10.1103/PhysRevLett.95.096101

PACS numbers: 68.60.–p, 64.75.+g

Interfaces between coexisting phases are ubiquitous in condensed matter. Nevertheless, a fundamental issue that is not fully understood [1–10] is the precise relation between the so-called “intrinsic interfacial profile” and the broadening caused by lateral fluctuations of the local interface position. Theories for interfacial profiles go back to van der Waals [11], Cahn and Hilliard [12], and others, and neglect these latter fluctuations, yielding the “intrinsic profile” only. This remains true for more sophisticated extensions of mean-field-type theories such as density functional theories of fluids [5] or self-consistent field theory of polymer blends [13].

Lateral interface fluctuations on large length scales are modeled as “capillary waves” [14–16]. For a free interface in three dimensions, these fluctuations lead to a divergent interfacial width. This divergence is cut off at large length scales either by the lateral size, L , of the system or by a correlation length, ξ_{\parallel} , which may stem from a potential acting on the interface (e.g., due to gravity or interaction with substrates [4,17–19]). Normally, ξ_{\parallel} is a function of film thickness D and, hence, a dependence on either L [4,10,20,21] or D [4,17–19] is seen in experiments [10,17,19] or simulations [4,18,21]. While these results agree with predictions based on capillary wave theory, they do not allow a meaningful estimation of the “intrinsic” interfacial width, w_0 , because the total apparent width, w , contains both contributions from the intrinsic profile as well as capillary wave broadening. Approximating the apparent profile by a convolution of the intrinsic profile with capillary waves, one obtains

$$w^2 = w_0^2 + k_B T / (4\gamma) \ln(L/B_0), \quad (1)$$

γ being the (long wavelength limit of the) interfacial stiffness [2,3] and B_0 a cutoff at short wavelengths. For fluid interfaces in three dimensions the value of γ agrees with the interface tension (i.e., the excess free energy of the interface per unit area), while in general γ refers to the free energy penalty for *deforming* the interface. Note that Eq. (1) only holds for $L \gg B_0$ because at short wave-

lengths also the wavelength dependence of the interfacial stiffness [5–7,9,22,23] matters. None of the quoted experiments and simulations were able to clearly identify w_0 , since data of w^2 as a function of L only yield $w_0^2 - k_B T (\ln B_0) / 4\gamma$, but not w_0 and B_0 separately [24].

Despite the apparent universality of this problem, systems exist for which the lateral interfacial fluctuations are suppressed by long-range interactions. In the present work, we demonstrate this effect by model calculations for a binary alloy (*A*, *B*) on a compressible lattice with long-range elastic correlations. While it has been common knowledge that elasticity plays a crucial role in phenomena like alloy formation [25] or surface reconstruction [26], its effect on interface fluctuations has so far not been noticed [27]. For a coherent binary alloy no capillary waves occur, and the intrinsic profile is readily observed. Since for solids strictly rigid lattices are anyway an idealization and for most phase transitions there will be some coupling between the order parameter and elastic degrees of freedom we expect in solids well-defined intrinsic interfacial profiles, unlike fluid interfaces.

Our model has been previously studied in the bulk [28] to describe the phase diagram of solid Si-Ge mixtures. Despite the difference in lattice parameters between these two elements, which both crystallize in the diamond lattice, one observes complete miscibility at high temperatures, while phase separation occurs at low temperatures. If the lattice were rigid, the transition would fall in the universality class [29] of the three-dimensional Ising model. The compressible system in the constant-pressure, semigrand canonical ensemble, however, clearly shows mean-field critical behavior, providing evidence for the importance of long-range elastic interactions [28]. This can be rationalized as follows: The order parameter couples directly to the fluctuations of the volume of the system or to the elastic strain. In contrast to the compressible Ising model [30] with strict spin-up/spin-down symmetry, one now has a correspondence between the mean volume and the mean order parameter (like for hydrogen in metals

[31]). This implies that one can also use the strain as the fundamental order parameter, as it is done in Cowley's [32] theory of structural phase transitions. There the transition is predicted to be a mean-field-like one because the order parameter couples only to the volume mode and the longitudinal phonons, with the former being intrinsically softer than the latter, due to the existence of a nonvanishing shear modulus [30,33]. Therefore the bulk mode already orders before any of the other modes has a chance to become critical.

The Keating-like [34] Hamiltonian of our model [28] is

$$\begin{aligned} \mathcal{H} = & \sum_{\langle i,j \rangle} (-JS_i S_j + E(S_i, S_j)[\mathbf{r}_{ij}^2 - R_0^2(S_i, S_j)]^2) \\ & + \sum_{\langle i,j,k \rangle} A(S_i, S_j, S_k)[\mathbf{r}_{ij} \cdot \mathbf{r}_{kj} \\ & + R_0(S_i, S_j)R_0(S_k, S_j)/3]^2, \end{aligned} \quad (2)$$

where the pseudospins $S_i = \pm 1$ represent *A* vs *B*, \mathbf{r}_{ij} is the bond vector between the sites *i* and *j*, $\sum_{\langle i,j \rangle}$ denotes a sum over nearest neighbors, and $\sum_{\langle i,j,k \rangle}$ denotes the sum over two nearest neighbor bonds *i, j* and *j, k* with common vertex at site *j*. The “exchange constant” of the Ising model is $J = 0.005$ eV [28], and the constants defining the energies $E(S_i, S_j)$ and $A(S_i, S_j, S_k)$ are given in Ref. [28]. The key feature of this model is that the two species prefer different bond lengths R_0 : $R_0(1, 1) = 2.352$ Å and $R_0(-1, -1) = 2.450$ Å, and $R_0(1, -1) = 2.401$ Å, respectively. If all three choices of R_0 were taken the same, a compressible lattice with no mismatch between *A* and *B* would result.

We choose a $L \times L \times D$ geometry with periodic boundary conditions in the *x, y* direction and two free $L \times L$ surfaces on which surface chemical potentials act, such that at $z = 0$ the *A*-rich and at $z = D$ the *B*-rich phase is preferred. Denoting the surfaces at $z = 0$ and $z = D$ with “(1)” and “(2)”, respectively, this additional part of the Hamiltonian [35] is

$$\begin{aligned} \mathcal{H}_{\text{surf}} = & -\mu_A^{(1)} \sum_{i \in (1)} \delta_{S_i, +1} - \mu_A^{(2)} \sum_{i \in (2)} \delta_{S_i, +1} \\ & - \mu_B^{(1)} \sum_{i \in (1)} \delta_{S_i, -1} - \mu_B^{(2)} \sum_{i \in (2)} \delta_{S_i, -1} \end{aligned} \quad (3)$$

with $\mu_B^{(1)} = \mu_A^{(2)} = 0$, $\mu_A^{(1)} = 0.0582$ eV, $\mu_B^{(2)} = 0.0418$ eV. This choice means that the left wall prefers *A* with the same strength with which the right wall prefers *B*. We apply the NpT ensemble.

The total number of particles is $N = 8L^2D$ because the diamond lattice consists of 8 interpenetrating simple cubic lattices whose lattice constant corresponds to the linear size of the diamond conventional cell. We choose $N_A = N_B = N/2$, and normally initialize the system such that particles for $0 \leq z \leq D/2$ are of type *A* and for $D/2 \leq z < D$ are of type *B* [36]. Applying moves in the constant-pressure ensemble, the concentration profile is equilibrated

by allowing for “spin exchange-type” of moves between arbitrary pairs of sites. The positions are equilibrated by trying to move a particle from its old position \mathbf{r}_i to a randomly chosen new position \mathbf{r}'_i within a small surrounding area of the old position [28,35]. In the surface plane, only lateral motions are permitted. To allow for faster equilibration, also nearest neighbor relaxation moves of the type proposed by Kelires [37] were implemented. Two sizes were utilized ($4 \times 4 \times 6$ and $8 \times 8 \times 12$) and between 3×10^6 and 10^7 Monte Carlo steps per site were used for the averaging. Temperatures studied were $k_B T = 0.005, 0.006$, and 0.007 eV [35], but here only the results for the lowest temperature are described. Parallel to the surfaces we observe an average lattice constant $a = 5.5307$ Å which is similar to the arithmetic mean of the lattice constant that would result for pure Si and pure Ge from the Keating potential [34], $\bar{a} = 5.5449$ Å.

Figure 1 shows our central result, namely, evidence that the interfacial profile is independent of both L and D . By analyzing subsystems of size $(B/4) \times (B/4) \times D$ instead of the full system $L \times L \times D$, we observe that there is practically no dependence on B , unlike the findings for the rigid Ising model [20,21], the lattice model for polymer blends [4], etc.,. Only when the sub-block linear dimension is reduced to the size of a few Å, as is the case for $B = 4$, does the interfacial profile sharpen. The behavior at higher temperatures is qualitatively similar [35].

We believe that this phenomenon can be explained as follows: Consider Fig. 2(a), where the analogous situation for a two-dimensional square lattice is shown. The pure species have the same type of unit cell (square), but different lattice spacings. In the coherent, demixed alloy the atom-atom distances parallel to the interface will assume

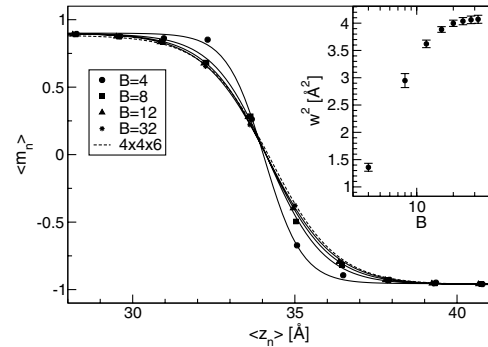


FIG. 1. Profile of the local magnetization $\langle m_n \rangle = \langle S_i \rangle_{i \in n}$ of the $8 \times 8 \times 12$ system for different block sizes B (values quoted in the key), shown by solid lines, and the total profile of the $4 \times 4 \times 6$ system (this would correspond to $B = 16$) as a dashed line. The symbols present the actual simulation data, while the curves are fits to a tanh profile which is the standard mean-field result for an intrinsic profile. Note that $\langle m_n \rangle$ is related to the concentration profile via $\phi(z) = (1 + \langle m_n \rangle)/2$. The inset shows the squared width vs B , choosing a logarithmic abscissa to show that there is *no* regime where $w^2 \propto \ln B$ holds, rather w^2 saturates at a finite value rather quickly.

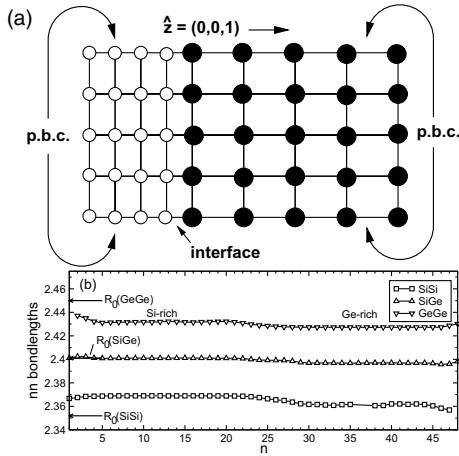


FIG. 2. (a) Qualitative sketch of a typical configuration of a coherent two-dimensional binary alloy with mismatch in the lattice spacing. The pure species both crystallize in a square lattice. (b) Distances in planes parallel to the interface (001) in Å vs layer index n for the $8 \times 8 \times 12$ system. The arrows indicate the ideal bond lengths R_0 used in the Keating potential.

some compromise value between the two optimum spacings for A and B throughout the system. In other words, none of these parallel bonds is relaxed—they are all either stretched or squeezed. Conversely, the bonds perpendicular to the interface are all relaxed, except for a few near the interface. We note that the approximation used in Fig. 2(a) (complete neglect of bond angle fluctuations, which must remain very limited as a result of the boundary conditions), has been put forward previously [38]. Obviously, this behavior implies that the introduction of the interface costs a free energy which does not scale as the area L^2 , but rather as the volume L^2D . This implies an infinite interfacial tension. It should be noted that the periodic boundary conditions correspond to the condition of coherency in the real alloy. These considerations show that coherency can only occur up to a certain length scale beyond which rupture of the network (incoherent phase coexistence) becomes more favorable. This latter phenomenon is well-known from metallurgy [39].

Furthermore, not only the introduction but also the deformation of an interface costs a free energy which scales as the volume, implying that the interfacial stiffness γ in Eq. (1) is infinite (proportional to the film thickness D), such that capillary waves are suppressed. This extensive free energy penalty for deformation can be shown within the framework of continuum elasticity theory [25]. For anisotropic elasticity (which is the case here), the elastic Hamiltonian can be written as a pairwise long-ranged strain-strain interaction. From this, one can show that the elastic free energy penalty for an A inclusion in a B matrix is proportional to the system volume [25], and depends on the shape of the inclusion. A shape change, however, is equivalent to deforming the interface. The effect of an extensive interfacial stiffness is qualitatively different from a mere modification of the capillary wave

spectrum (e.g., a cutoff with a concomitant correlation length ξ_{\parallel}); interface fluctuations are eliminated because their energy is infinitely larger than $k_B T$.

Figure 2(b) shows the layer-layer distances of the planes parallel to the interface and demonstrates that the configurations sketched in Fig. 2(a) are indeed typical for our system. It should, however, be noted that in our case (diamond lattice) the main distortion does not come from the bond lengths, but rather from the local bond angles. The A - A , B - B , and A - B nearest neighbor distances essentially retain their values independently of z (data not shown), while the bond angles deviate substantially from the ideal tetrahedron value (Fig. 3). This distortion occurs throughout the sample and stores most of the elastic energy cost of the interface.

This picture is further corroborated by simulations in the semigrand canonical ensemble. Here, we find that a structure of the type shown in Figs. 1–3 generally is unstable; rather the interface gets bound either to the boundary at $z = 0$ or at $z = D$ (Fig. 4) [40]. Unlike the Ising model on a rigid lattice our model does not exhibit an interface delocalization transition where the interface unbinds from one of the boundaries and moves towards the center of the film [18]. Rather the interface stays bound to one of the walls up to the critical temperature where the film disorders ($k_B T_c \approx 0.0175$ eV, note that in the canonical ensemble T_c is expected to be substantially smaller [38]). This lack

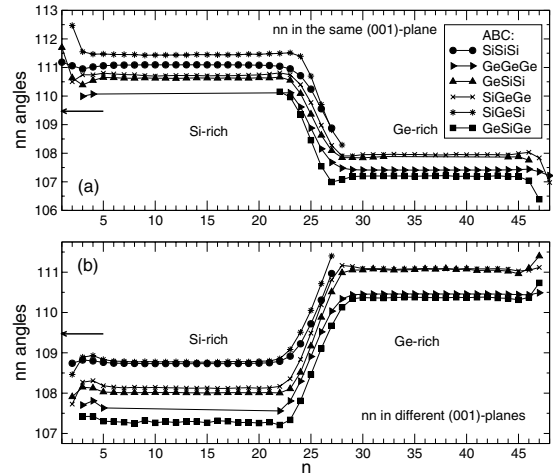


FIG. 3. Angles between nearest neighbors (nn) termed A , B , and C , B being the atom in vertex position, plotted vs the layer index in the z direction across a $8 \times 8 \times 12$ system. The layer index refers to that plane where the vertex atom sits. In the upper panel (a) the two nearest neighbors A and C are located in the same (001)-plane, while in the lower panel (b) the two nearest neighbors A and C are located in different (001)-planes (one with layer index $n - 1$ and one with layer index $n + 1$, if the vertex atom has layer index n). The arrows mark the angle $\theta = 109.47^\circ$ of the perfect tetrahedron. The data points correspond to an average over 2705 configurations taken at intervals of 10^3 Monte Carlo steps. Only angles appearing on average at least once per plane are shown. Errors are smaller than the size of the symbols.

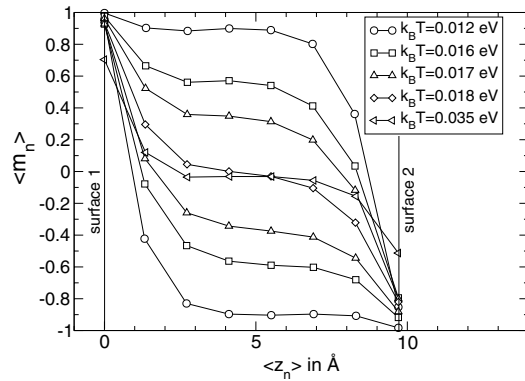


FIG. 4. Magnetization profiles $\langle m_n \rangle$ vs plane position $\langle z_n \rangle$ across the film, using a very thin film of size $8 \times 8 \times 2$, at various temperatures as indicated. The z coordinates of the two surfaces where the boundary fields act are shown by vertical straight lines. For $k_B T < 0.018$ eV two profiles are shown for each temperature, corresponding to different signs of the total magnetization $M = \sum_i S_i$.

of interface delocalization, which would only be expected above the temperature of a wetting transition, is consistent with the finding [41] that in adsorbed solid layers strains caused by the substrate potential prevent complete wetting of a solid film, and with the special role of the volume mode which explains the system's mean-field-like criticality in the bulk.

In summary, we have shown that interfaces between coexisting phases on compressible lattices behave very differently from their counterparts on rigid lattices or fluid mixtures: capillary waves are essentially suppressed, an intrinsic interfacial profile with mean-field character is easily found, but interface formation is intimately linked to large-scale elastic distortions of the lattice, and therefore it is generally unfavorable to form planar interfaces over large length scales separating large homogeneous domains. The consequences of these observations are far from being fully explored.

This work was supported in part by the Deutsche Forschungsgemeinschaft (DFG) under Grants No. Bi314/17 and No. TR6/A5. Stimulating discussions with D.P. Landau and F. Tavazza are gratefully acknowledged.

[1] B. Widom, in *Phase Transitions and Critical Phenomena*, edited by C. Domb and M.S. Green (Academic, New York, 1972), Vol. 2.
 [2] J.S. Rowlinson and B. Widom, *Molecular Theory of Capillarity* (Clarendon, Oxford, 1982).
 [3] D. Jasnow, Rep. Prog. Phys. **47**, 1059 (1984).
 [4] A. Werner *et al.*, J. Chem. Phys. **107**, 8175 (1997).
 [5] K.R. Mecke and S. Dietrich, Phys. Rev. E **59**, 6766 (1999).
 [6] E. Chacón and P. Tarazona, Phys. Rev. Lett. **91**, 166103 (2003).
 [7] M. Müller and L.G. MacDowell, Macromolecules **33**, 3902 (2000).

[8] K. Binder and M. Müller, Int. J. Mod. Phys. C **11**, 1093 (2000).
 [9] A. Milchev and K. Binder, Europhys. Lett. **59**, 81 (2002).
 [10] D. Aarts, M. Schmidt, and H.N.W. Lekkerkerker, Science **304**, 847 (2004).
 [11] J.D. van der Waals, Verh. K. Ned. Akad. Wet., Afd. Natuurkd., Eerste Reeks **1**, 8 (1893).
 [12] J.W. Cahn and J.E. Hilliard, J. Chem. Phys. **28**, 258 (1958).
 [13] E. Helfand and Y. Tagami, J. Chem. Phys. **56**, 3592 (1972).
 [14] F.P. Buff, R.A. Lovett, and F.H. Stillinger, Phys. Rev. Lett. **15**, 621 (1965).
 [15] J.D. Weeks, J. Chem. Phys. **67**, 3106 (1977).
 [16] D. Bedeaux and J.D. Weeks, J. Chem. Phys. **82**, 972 (1985).
 [17] M. Sferrazza *et al.*, Phys. Rev. Lett. **78**, 3693 (1997).
 [18] K. Binder, D.P. Landau, and A.M. Ferrenberg, Phys. Rev. Lett. **74**, 298 (1995); Phys. Rev. E **51**, 2823 (1995).
 [19] T. Kerle, J. Klein, and K. Binder, Phys. Rev. Lett. **77**, 1318 (1996); Eur. Phys. J. B **7**, 401 (1999).
 [20] K.K. Mon *et al.*, Phys. Rev. B **42**, 545 (1990).
 [21] F. Schmid and K. Binder, Phys. Rev. B **46**, 13565 (1992).
 [22] D.X. Li *et al.*, Phys. Rev. Lett. **92**, 136102 (2004).
 [23] A.O. Parry and C.J. Boulter, J. Phys. Condens. Matter **6**, 7199 (1994).
 [24] If $\xi_{\parallel} < L$, L in Eq. (1) needs to be replaced by ξ_{\parallel} .
 [25] P. Fratzl, O. Penrose, and J.L. Lebowitz, J. Stat. Phys. **95**, 1429 (1999).
 [26] P. Müller and A. Saul, Surf. Sci. Rep. **54**, 157 (2004).
 [27] J.D. Weeks, D. Bedeaux, and B.J.A. Zielinska, J. Chem. Phys. **80**, 3790 (1984) study suppression of capillary waves in a mathematical model for a *fluid*, with no direct relation to the physical origin of the long-range interaction.
 [28] B. Dünweg and D.P. Landau, Phys. Rev. B **48**, 14182 (1993).
 [29] M.E. Fisher, Rev. Mod. Phys. **46**, 597 (1974).
 [30] A.I. Larkin and S.A. Pikin, Sov. Phys. JETP **29**, 891 (1969).
 [31] H. Wagner and H. Horner, Adv. Phys. **23**, 587 (1974).
 [32] R.A. Cowley, Phys. Rev. B **13**, 4877 (1976).
 [33] S.A. Pikin, Physica (Amsterdam) **194A**, 352 (1993).
 [34] P.N. Keating, Phys. Rev. **145**, 637 (1966).
 [35] B.J. Schulz, Ph.D. thesis, Universität Mainz, 2004.
 [36] In several cases it was checked that a different starting condition yields equivalent results.
 [37] P.C. Kelires, Phys. Rev. Lett. **75**, 1114 (1995).
 [38] E.M. Vandeworp and K.E. Newman, Phys. Rev. B **52**, 4086 (1995); **55**, 14222 (1997).
 [39] R.D. Doherty, in *Physical Metallurgy*, edited by R.W. Cahn and P. Haasen (Elsevier, Amsterdam, 1983), 3rd ed., p. 933.
 [40] We only allowed the lateral linear dimensions to fluctuate, while the thickness of the film was fixed to a constant value, as if the sample were clamped into a workbench (the lattice constant in z direction was chosen to be the arithmetic mean of pure Si and pure Ge). Allowing the film thickness to fluctuate too, we observe similar behavior.
 [41] F.T. Gittes and M. Schick, Phys. Rev. B **30**, 209 (1984).